Open Journal of Applied Sciences, 2025, 15(10), 3113-3130
https://www.scirp.org/journal/ojapps
ISSN Online: 2165-3925
ISSN Print: 2165-3917

Liquidus Modelling of SiO_2-Na_2O-CaO Ternary Mixtures Vitrifiable by Mixing Plane

Péyokoh Roger Thio[1*], Mohamed Karamoko[1], Kouassi Bruno Koffi[1], Kouadio Denis Konan[1], Cyrille N'dri Kouakou[2], Ardjouma Ganon[2]

[1]Mechanics and Materials Science Laboratory, National Polytechnic Institute Félix Houphouët-Boigny (INP-HB), Yamoussoukro, Côte d'Ivoire
[2]Mathematics and New Information Technologies, National Polytechnic Institute Félix Houphouët-Boigny (INP-HB), Yamoussoukro, Côte d'Ivoire
Email: *peyokoh.thio@inphb.ci

How to cite this paper: Thio, P.R., Karamoko, M., Koffi, K.B., Konan, K.D., Kouakou, C.N. and Ganon, A. (2025) Liquidus Modelling of SiO_2-Na_2O-CaO Ternary Mixtures Vitrifiable by Mixing Plane. *Open Journal of Applied Sciences*, **15**, 3113-3130.
https://doi.org/10.4236/ojapps.2025.1510205

Received: July 14, 2025
Accepted: October 17, 2025
Published: October 20, 2025

Abstract

In this study, melting temperature modeling was carried out for SiO_2-Na_2O-CaO ternary vitrifiable oxide mixtures, based on literature data and the results of our experimental tests. The aim of this modeling is to determine a mathematical model for predicting the melting temperature of vitrifiable mixtures composed of the oxides of silicon, sodium, and calcium using the proportions of these to produce silica glass. First, the mathematical approach with first-order, second-order, synergistic third order and full third-order models was implemented. Secondly, the experimental approach was used to validate a model for estimating the liquidus of SiO_2-Na_2O-CaO ternary mixtures through melting tests. The accuracy evaluated with the coefficient of determination (R^2) of the full third-order model selected is 0.9908. Based on the liquidus model obtained, a ternary diagram was proposed to facilitate the determination of temperatures as a function of ternary mixture compositions. In addition, an algorithm has been developed based on this model to facilitate its use.

Keywords

Soda-Lime-Silica Glass, Ternary Vitrifiable Oxide Mixtures, Melting Temperature Modeling, Ternary Diagram

1. Introduction

The thermodynamic study of the binary systems Na_2O-SiO_2 and CaO-SiO_2 as well as the ternary system SiO_2-Na_2O-CaO has enabled the construction of partial phase diagrams of these systems (**Figure 1**) [1]-[3]. The ternary system has been partially constructed by several authors (**Figure 1**). The most recent publication of this ternary diagram by Zhang Z. *et al.* is a projection of the SiO_2-Na_2O-CaO ternary diagram, whose vertices are SiO_2, $80Na_2O$-$20SiO_2$ and 80Cao-$20SiO_2$ [4]-[6]. The industrial production of soda-lime glass is made with a silica mass proportion of between 60% and 80%. The melting temperature of this production is in the range 1450˚C to 1550˚C, with the addition of cullet (recycled glass) and Na_2O as flux [7].

The melting of SiO_2-Na_2O-CaO mixtures is an energy-intensive process. In addition to the high energy consumption, which limits the number of tests that can be carried out, the chemical and physical mechanisms occurring at high temperatures are becoming complex from a thermodynamic point of view. In this context, determining the liquidus of vitrifiable mixtures as a function of composition remains a key area of research [8].

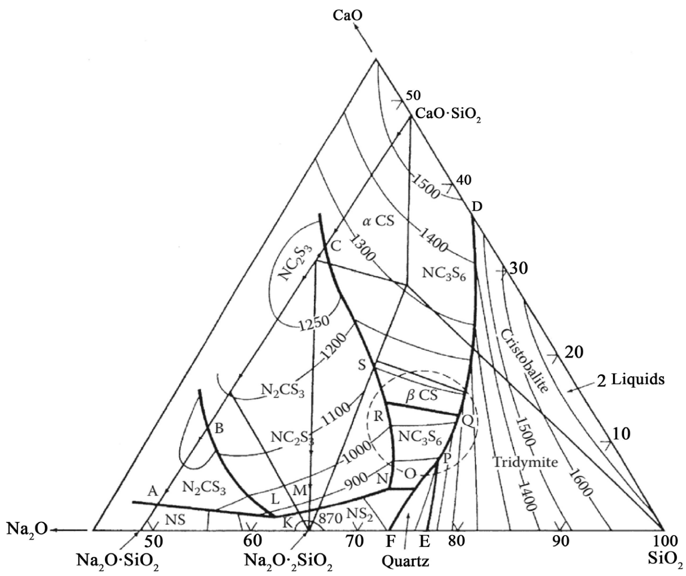

Figure 1. Ternary diagram liquidus SiO_2-Na_2O-CaO [2].

In this study, we address the problem of melting ternary SiO_2-Na_2O-CaO mixtures from a mathematical perspective using the mixing plane approach. This concept allows for visualization of how combinations of these components influence melting behavior and phase formation. The aim of this approach is to establish a mathematical model of the melting temperature (liquidus) as a function of the proportion of soda, silica and lime in each mixture. The data used and quoted in this study come from the literature and concern studies of this ternary system from the thermodynamic point of view. We then carried out test trials to validate the model obtained.

2. Materials and Methods

2.1. Study Data

The data used come from several publications. The phase equilibrium diagram of the SiO_2-Na_2O-CaO system established by Rankin, Wright, Greig and Clifton provides the liquidus of silica (1723˚C) and lime (2570˚C) [2] [3]. The phase diagram of the SiO_2-Na_2O-CaO system from the FACT database provides the liquidus of soda ash (1132˚C) [4] [5]. The data is collated by considering the vitrification tests of said ternary mixture. A table summarizing the data is drawn up. This table is used to determine the matrices for the modeling phase. A starting matrix whose columns are the constituents of the ternary system. A column matrix of the melting temperatures of the respective mixtures is also constructed.

2.2. Characterization Model

We are looking for a mathematical expression of the correlations between compositions and melting temperature. The mixture models described in Chapter 4 are determined for this phase data. These range from the first-order model to the third-order synergistic model. The mathematical temperature functions of these models are listed below [9]-[11].

First-order model

$$\hat{T}_1\left(^{\circ}\mathrm{C}\right)=\sum_{i=1}^{3}b_i x_i$$

Second-order model

$$\hat{T}_2\left(^{\circ}\mathrm{C}\right)=\sum_{i=1}^{m}b_i x_i+\sum\sum_{i<j}b_{ij}x_i x_j$$

Complete third-order model

$$\hat{T}_{3,C}\left(^{\circ}\mathrm{C}\right)=\sum_{i=1}^{m}b_i x_i+\sum\sum_{i<j}b_{ij}x_i x_j+\sum\sum_{i<j}b_{ij}x_i x_j\left(x_i-x_j\right)+\sum\sum_{i<j}\sum b_{ijk}x_i x_j x_k$$

Synergistic third-order model

$$\hat{T}_{3,S}\left(^{\circ}\mathrm{C}\right)=\sum_{i=1}^{m}b_i x_i+\sum\sum_{i<j}b_{ij}x_i x_j+\sum\sum_{i<j}\sum b_{ijk}x_i x_j x_k$$

For these models, the parameters have the following characteristics.

$$b_i, b_{ij}, b_{ijk}, T\left(^{\circ}\mathrm{C}\right)\in\mathbb{R}$$

$$x_i, x_j, x_k\in\left\{\%\mathrm{SiO_2};\%\mathrm{Na_2O};\%\mathrm{CaO}\right\}\ \text{et}\ x_i, x_j, x_k\in\left[0;1\right]$$

The coefficients b_i, b_{ij}, b_{ijk} of the component proportions x_i, $x_i x_j$ and $x_i x_j x_k$ respectively represent their influence on the melting temperature [9]-[11].

2.3. Data Set Separation

Empirical analysis has shown that the best results are obtained by allocating 20% - 30% of the initial data points for the tests and using the remaining 70% - 80% for the training set [12]-[14]. Knowing that we have 46 data points, this means that we'll have around 9 to 14 points for the tests and around 32 to 37 points for the training set. This distribution will enable us to test the performance of our model on a separate dataset from the one on which it was trained, which is essential for assessing its ability to generalize to new data. We will then be able to adjust our model according to the performance observed on the test set to optimize its performance on future datasets.

2.4. Statistical Evaluation

The statistical study is carried out to assess the quality of the model through the coefficient of determination (correlation). This coefficient is defined by the expression below

$$R^2 = \frac{SSR}{SST} = 1 - \frac{SSE}{SST}$$

With

Total sum of squares:

$$SST = \sum_{i=1}^{n}\left(T_i^*\right)^2 = \sum_{i=1}^{n}\left(T_i - \bar{T}\right)^2$$

Sum of squares due to error

$$SSE = \sum_{i=1}^{n}\left(T_i - \hat{T}_i\right)^2$$

sum of squares due to regression

$$SSR = \sum_{i=1}^{n}\left(\hat{T}_i - \bar{T}\right)^2$$

The closer R^2 is to 1, the "closer" the fitted model is to the observed responses. A classic threshold is to look for models for $R^2 \geq 0.9500$. This procedure enables us to assess the accuracy of the mathematical model. This procedure enables us to assess the accuracy of the mathematical model [9].

2.5. Melting Test for Vitrifiable Mixtures

Mixtures of the ternary SiO_2-Na_2O-CaO system were prepared and melted to validate the best model obtained in terms of the correlation coefficient. These mixtures were melted at the temperatures predicted by the model. Micrography of the glass samples obtained is used to validate the model by observing the melting state of the test mixtures. The silica raw material is collected locally in the Maféré area, Côte d'Ivoire [15].

In view of the equipment available in our laboratory, we have chosen melting temperatures below 1250˚C. This temperature limit is set according to our furnace, whose maximum temperature is 1280˚C. Using this temperature, we generate ternary system mixtures [16].

Melt tests are carried out with a powdered siliceous raw material with a granularity of between 80 µm and 100 µm (**Figure 2** and **Figure 3**). This particle size is similar to that used by Marlind Daud and Mahadi Abu in their work on soda-lime glass production [17].

Figure 2. Grades of treated silica sand from Maféré, Côte d'Ivoire.

(a) (b)

Figure 3. Silica granulometric class used for the production of silica glass. (a) silica powder <80 µm; (b) silica with granularity between 80 µm and 100 µm.

Sodium and calcium are supplied to the mixtures in a solid state (powder) through their carbonates. Grynberg's work on the ternary system SiO_2-Na_2O-CaO showed the possibility of using these carbonates for the production of soda-lime glass [7] [17]. **Figure 4** and **Figure 5** below illustrate the sodium and calcium carbonate labels used in our experiment.

(a) (b)

Figure 4. (a) Sodium carbonate; (b) Calcium carbonate.

The 200 grams mixtures are introduced into crucibles for melting (**Figure 5**). The temperature rise from ambient to target temperature takes about an hour.

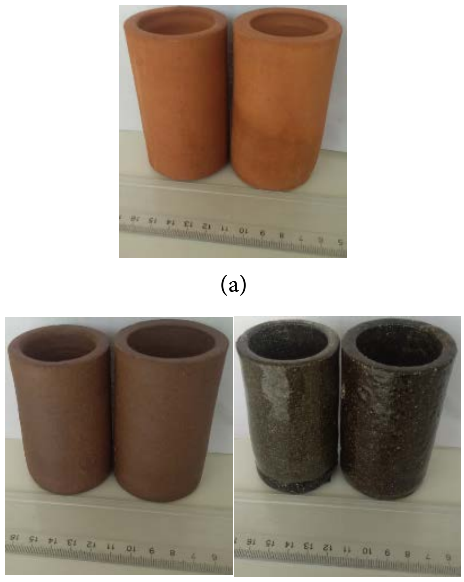

(a)

(b) (c)

Figure 5. Crucibles used for melting test mixes. (a) Crucible manufactured at the Katiola ceramic center; (b) Crucible in (a) pre-fired at 1250˚C; (c) Crucible in (a) after a vitrifiable mix melting test.

3. Results and Discussion

The results of this study concern first the synthesis of melting temperatures of vitrifiable mixtures. The data are taken from the literature and the authors' own work. Then, mathematical models are determined for the predictive calculation of the melting temperature of SiO_2-Na_2O-CaO ternary mixtures. Finally, the quality of the mathematical models established is assessed.

3.1. Synthesis of SiO_2-Na_2O-CaO Ternary Mixtures

Several mixtures with varying compositions of silica, soda ash and lime have been identified. Table 1 summarizes these mixtures and their respective melting temperatures. Compositions are considered in the interval [0; 1] and temperatures are in degrees Celsius.

Table 1. Compositions of SiO_2-Na_2O-CaO mixtures.

N˚	SiO_2	Na_2O	CaO	T (˚C)	Mixing type	N˚	SiO_2	Na_2O	CaO	T (˚C)	Mixing type
1	0.00	1.00	0.00	1132	pure	24	0.45	0.07	0.48	1325	Ternary
2	0.00	0.00	1.00	2570	pure	25	0.46	0.08	0.46	1303	Ternary
3	0.33	0.00	0.67	2130	binary	26	0.46	0.12	0.42	1300	Ternary
4	0.39	0.20	0.41	1428	Ternary	27	0.46	0.11	0.43	1315	Ternary
5	0.39	0.21	0.40	1425	Ternary	28	0.47	0.08	0.45	1325	Ternary
6	0.41	0.22	0.37	1315	Ternary	29	0.47	0.09	0.44	1317	Ternary
7	0.41	0.24	0.35	1292	Ternary	30	0.47	0.11	0.42	1285	Ternary

Continued

8	0.41	0.22	0.37	1300	Ternary	31	0.47	0.13	0.40	1305	Ternary
9	0.41	0.25	0.34	1300	Ternary	32	0.47	0.14	0.39	1310	Ternary
10	0.42	0.11	0.47	1325	Ternary	33	0.48	0.12	0.41	1287	Ternary
11	0.42	0.10	0.48	1320	Ternary	34	0.50	0.50	0.00	1400	binary
12	0.42	0.25	0.33	1300	Ternary	35	0.50	0.00	0.50	1544	binary
13	0.43	0.23	0.35	1300	Ternary	36	0.62	0.23	0.15	1450	Ternary
14	0.43	0.08	0.49	1325	Ternary	37	0.74	0.13	0.13	1450	Ternary
15	0.43	0.09	0.48	1320	Ternary	38	0.74	0.16	0.10	1450	Ternary
16	0.43	0.10	0.46	1305	Ternary	39	0.74	0.20	0.06	1450	Ternary
17	0.44	0.21	0.36	1295	Ternary	40	0.75	0.15	0.10	1500	Ternary
18	0.44	0.07	0.50	1330	Ternary	41	0.78	0.11	0.11	1450	Ternary
19	0.45	0.20	0.36	1310	Ternary	42	0.78	0.14	0.08	1450	Ternary
20	0.45	0.07	0.48	1305	Ternary	43	0.78	0.17	0.05	1450	Ternary
21	0.45	0.09	0.46	1310	Ternary	44	0.80	0.10	0.10	1500	Ternary
22	0.45	0.17	0.38	1317	Ternary	45	0.80	0.15	0.05	1500	Ternary
23	0.45	0.22	0.33	1300	Ternary	46	1.00	0.00	0.00	1723	pure

Source*: [2]-[5] [7] [8] [16] [17].

The majority of SiO_2-Na_2O-CaO mixtures studied in the literature contain at most 80% silica [4] [5] [7] [18]. **Figure 6** below illustrates the silica proportion as a function of temperature of the blends used for modeling. The silica proportion of ternary mixtures ranges from 0.39 to 0.8 for laboratory tests and industrial production. The limit of 80% silica in blends is linked to the high melting temperature of silica (1723˚C). In **Figures 6-8**, the letters C and B are used to identify pure bodies and binary mixtures (mixtures of two components) respectively. In these figures, the areas circled with the letter T within these circles represent ternary mixtures. In ternary mixtures, the proportion of flux (sodium oxide) typically ranges from 5% to 25% (**Figure 7**), while the stabilizer (calcium oxide) content varies between 4% and 50% (**Figure 8**).

3.2. Liquidus Determination Model

The data in **Table 1** above have been used to establish the mathematical expressions below $T\left(^{\circ}\mathrm{C}\right)=f\left(\%\mathrm{SiO}_2;\%\mathrm{Na}_2\mathrm{O};\%\mathrm{CaO}\right)$. These are linear expressions of the components of the ternary system. Models from first-order mixtures to third-order synergistic models were determined. The accuracy of the models obtained was assessed.

3.2.1. First-Order Model

The first-order polynomial model adapted to the study of mixtures, for 3 components, is given by the expression below.

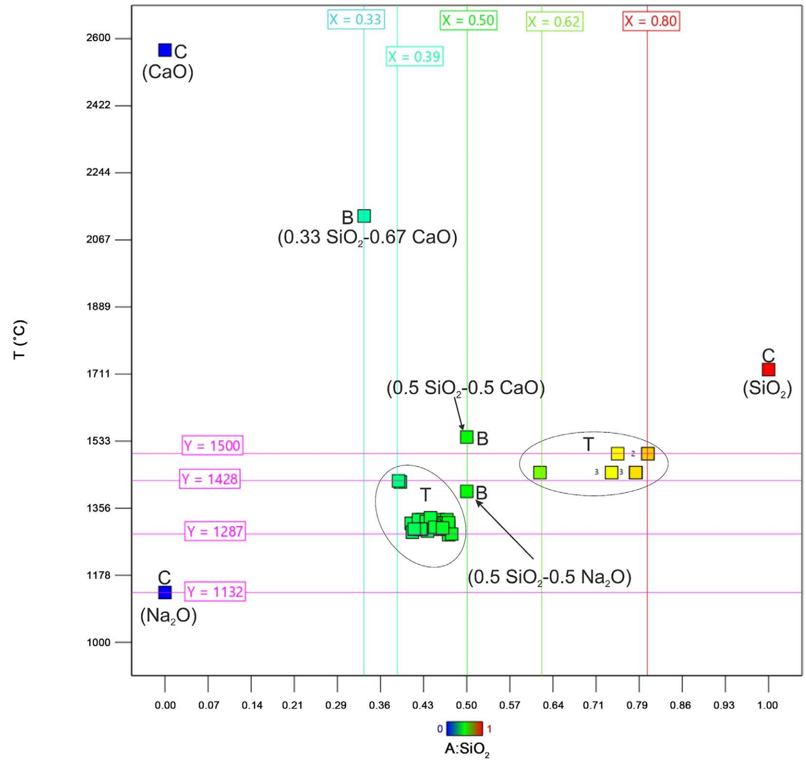

Figure 6. Mixture type as a function of silica proportion. B: binary mixture; C: pure substance; T: ternary mixture.

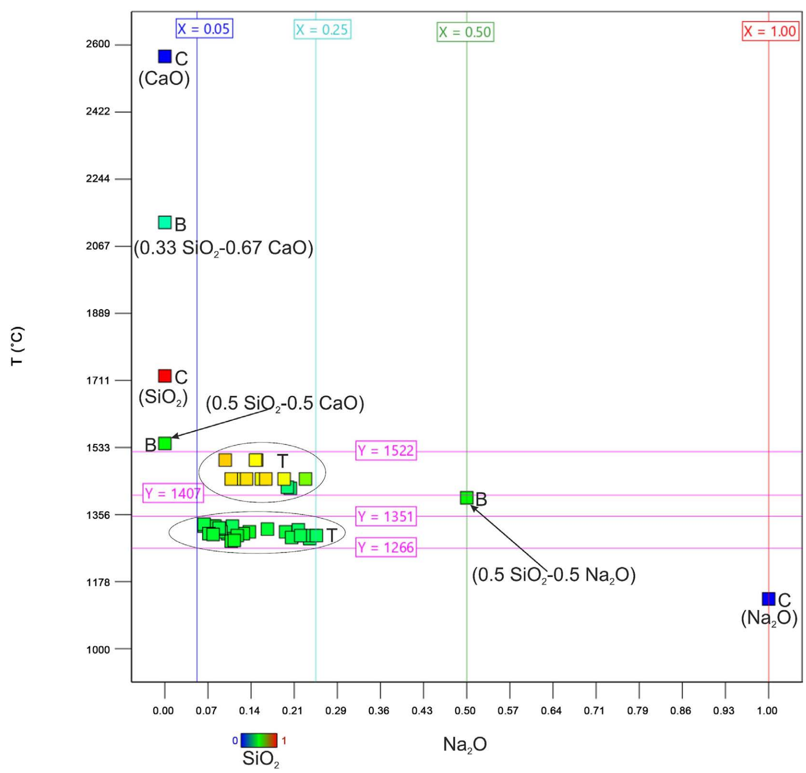

Figure 7. Temperature range of ternary mixtures as a function of the proportion of silica and Na_2O. B: binary mixture; C: pure substance; T: ternary mixture.

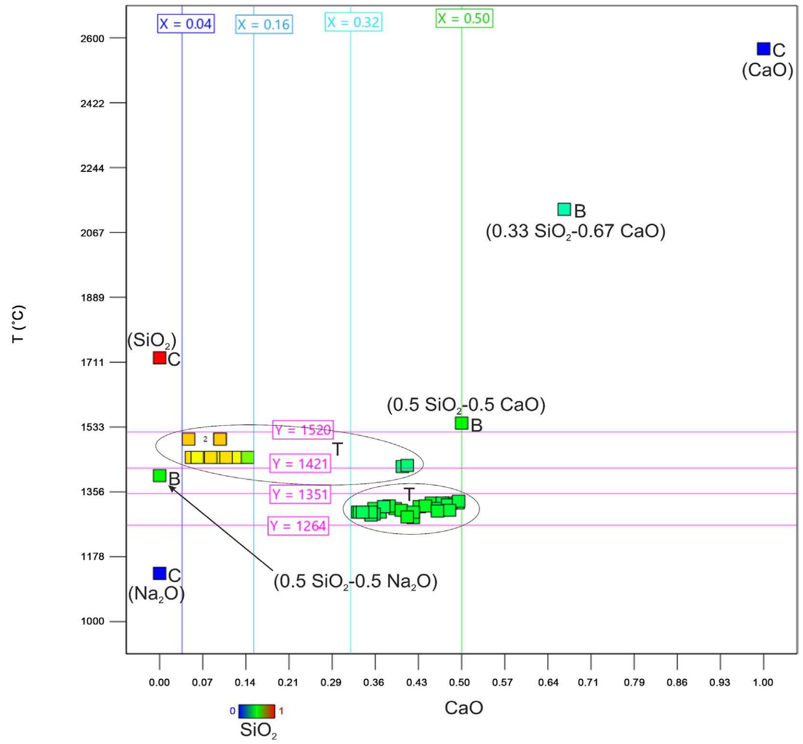

Figure 8. Temperature range of ternary mixtures as a function of the proportion of silica and CaO. B: binary mixture; C: pure substance; T: ternary mixture.

$$\hat{T}_1(^\circ\text{C}) = \sum_{i=1}^{3} b_i x_i$$

$$b_i, T(^\circ\text{C}) \in \mathbb{R}$$

$$x_i \in \{\%\text{SiO}_2; \%\text{Na}_2\text{O}; \%\text{CaO}\} \text{ and } x_i \in [0;1]$$

In detail

$$\hat{T}_1(^\circ\text{C}) = b_{\text{SiO}_2} x_{\text{SiO}_2} + b_{\text{Na}_2\text{O}} x_{\text{Na}_2\text{O}} + b_{\text{CaO}} x_{\text{CaO}}$$

$$\hat{T}_1(^\circ\text{C}) = 1305.69 \cdot x_{\text{SiO}_2} + 994.45 \cdot x_{\text{Na}_2\text{O}} + 1710.48 \cdot x_{\text{CaO}}$$

The quality of the polynomial $\hat{T}_1(^\circ\text{C})$ is given by its coefficient of determination. This coefficient of the first-order polynomial is very low compared with the reference ($R^2 = 0.2082 < 0.9500$).

3.2.2. Second-Order Model

The second-order polynomial model adapted to the study of mixtures, for 3 components, is given by $\hat{T}_2(^\circ\text{C})$.

$$\hat{T}_2(^\circ\text{C}) = \sum_{i=1}^{3} b_i x_i + \sum_{i<j}\sum b_{ij} x_i x_j$$

$$b_i, b_{ij}, T(^\circ\text{C}) \in \mathbb{R}$$

$$x_i, x_j \in \{\%\text{SiO}_2; \%\text{Na}_2\text{O}; \%\text{CaO}\} \text{ et } x_i, x_j \in [0;1]$$

In detail

$$\hat{T}_2\left({}^{\circ}\mathrm{C}\right)=b_{\mathrm{SiO_2}}x_{\mathrm{SiO_2}}+b_{\mathrm{Na_2O}}x_{\mathrm{Na_2O}}+b_{\mathrm{CaO}}x_{\mathrm{CaO}}+b_{\mathrm{SiO_2.Na_2O}}x_{\mathrm{SiO_2.Na_2O}}$$
$$+b_{\mathrm{SiO_2.CaO}}x_{\mathrm{SiO_2.CaO}}+b_{\mathrm{Na_2O.CaO}}x_{\mathrm{Na_2O.CaO}}$$

$$\hat{T}_2\left({}^{\circ}\mathrm{C}\right)=1662.1\cdot x_{\mathrm{SiO_2}}+1141.45\cdot x_{\mathrm{Na_2O}}+2644.36\cdot x_{\mathrm{CaO}}$$
$$+125.392\cdot x_{\mathrm{SiO_2.Na_2O}}-2729.23\cdot x_{\mathrm{SiO_2.CaO}}-3070.31\cdot x_{\mathrm{Na_2O.CaO}}$$

The quality of the polynomial $\hat{T}_2\left({}^{\circ}\mathrm{C}\right)$ is given by its coefficient of determination. This coefficient of the second-order polynomial is lower than the reference ($R^2 = 0.8805 < 0.9500$).

3.2.3. Complete Third-Order Model

The third-order polynomial model adapted to the study of mixtures, for $m = 3$ components, is given by $\hat{T}_{3,C}\left({}^{\circ}\mathrm{C}\right)$.

$$\hat{T}_{3,C}\left({}^{\circ}\mathrm{C}\right)=\sum_{i=1}^{3}b_i x_i+\sum\sum_{i<j}b_{ij}x_i x_j+\sum\sum_{i<j}a_{ij}x_i x_j\left(x_i-x_j\right)+\sum\sum_{i<j}\sum b_{ijk}x_i x_j x_k$$

$$b_i, b_{ij}, a_{ij}, b_{ijk}, T\left({}^{\circ}\mathrm{C}\right)\in\mathbb{R}$$

$$x_i, x_j, x_k\in\left\{\%\mathrm{SiO_2};\%\mathrm{Na_2O};\%\mathrm{CaO}\right\}\text{ and }x_i, x_j, x_k\in\left[0;1\right]$$

In detail

$$\hat{T}_{3,C}\left({}^{\circ}C\right)=b_{\mathrm{SiO_2}}x_{\mathrm{SiO_2}}+b_{\mathrm{Na_2O}}x_{\mathrm{Na_2O}}+b_{\mathrm{CaO}}x_{\mathrm{CaO}}+b_{\mathrm{SiO_2.Na_2O}}x_{\mathrm{SiO_2.Na_2O}}$$
$$+b_{\mathrm{SiO_2.CaO}}x_{\mathrm{SiO_2.CaO}}+b_{\mathrm{Na_2O.CaO}}x_{\mathrm{Na_2O.CaO}}+b_{\mathrm{SiO_2.Na_2O.CaO}}x_{\mathrm{SiO_2.Na_2O.CaO}}$$
$$+b_{\mathrm{SiO_2.Na_2O(SiO_2\text{-}Na_2O)}}x_{\mathrm{SiO_2.Na_2O(SiO_2\text{-}Na_2O)}}+b_{\mathrm{SiO_2.CaO(SiO_2\text{-}CaO)}}x_{\mathrm{SiO_2.CaO(SiO_2\text{-}CaO)}}$$
$$+b_{\mathrm{Na_2O.CaO(Na_2O\text{-}CaO)}}x_{\mathrm{Na_2O.CaO(Na_2O\text{-}CaO)}}$$

$$\hat{T}_{3,C}\left({}^{\circ}\mathrm{C}\right)=1726.15\cdot x_{\mathrm{SiO_2}}+1132.2\cdot x_{\mathrm{Na_2O}}+2572.46\cdot x_{\mathrm{CaO}}$$
$$-136.163\cdot x_{\mathrm{SiO_2.Na_2O}}-2479.67\cdot x_{\mathrm{SiO_2.CaO}}-10511\cdot x_{\mathrm{Na_2O.CaO}}$$
$$+25264\cdot x_{\mathrm{SiO_2.Na_2O.CaO}}-230.175\cdot x_{\mathrm{SiO_2.Na_2O(SiO_2\text{-}Na_2O)}}$$
$$-4790.55\cdot x_{\mathrm{SiO_2.CaO(SiO_2\text{-}CaO)}}+16880.8\cdot x_{\mathrm{Na_2O.CaO(Na_2O\text{-}CaO)}}$$

The coefficient of determination of the polynomial $\hat{T}_{3,C}\left({}^{\circ}\mathrm{C}\right)$ is $R^2 = 0.9908$. This value of the coefficient is greater than the reference $R^2 = 0.9908 > 0.9500$).

3.2.4. Synergistic Model of Third Order

The third-order synergetic polynomial model adapted to the study of mixtures, for $m = 3$ components, is given by $\hat{T}_{3,S}\left({}^{\circ}\mathrm{C}\right)$.

$$\hat{T}_{3,S}\left({}^{\circ}\mathrm{C}\right)=\sum_{i=1}^{3}b_i x_i+\sum\sum_{i<j}b_{ij}x_i x_j+\sum\sum_{i<j}\sum b_{ijk}x_i x_j x_k$$

$$b_i, b_{ij}, b_{ijk}, T\left({}^{\circ}\mathrm{C}\right)\in\mathbb{R}$$

$$x_i, x_j, x_k\in\left\{\%\mathrm{SiO_2};\%\mathrm{Na_2O};\%\mathrm{CaO}\right\}\text{ and }x_i, x_j, x_k\in\left[0;1\right]$$

In detail

$$\hat{T}_{3,S}\left({}^{\circ}\mathrm{C}\right)=b_{\mathrm{SiO_2}}x_{\mathrm{SiO_2}}+b_{\mathrm{Na_2O}}x_{\mathrm{Na_2O}}+b_{\mathrm{CaO}}x_{\mathrm{CaO}}+b_{\mathrm{SiO_2.Na_2O}}x_{\mathrm{SiO_2.Na_2O}}$$
$$+b_{\mathrm{SiO_2.CaO}}x_{\mathrm{SiO_2.CaO}}+b_{\mathrm{Na_2O.CaO}}x_{\mathrm{Na_2O.CaO}}+b_{\mathrm{SiO_2.Na_2O.CaO}}x_{\mathrm{SiO_2.Na_2O.CaO}}$$

$$\hat{T}_{3,S}(°C) = 1678.52 \cdot x_{SiO_2} + 1136.42 \cdot x_{Na_2O} + 2637.32 \cdot x_{CaO} + 193.998 \cdot x_{SiO_2.Na_2O} - 2697.82 \cdot x_{SiO_2.CaO} - 309.294 \cdot x_{Na_2O.CaO} - 6826.57 \cdot x_{SiO_2.Na_2O.CaO}$$

The quality of the polynomial $\hat{T}_{3,S}(^\circ C)$ is given by its coefficient of determination. This coefficient of the second-order polynomial is lower than the reference ($R^2 = 0.8820 < 0.9500$).

From the above, the best model is the complete third-order model. Using the mathematical expression of the complete third-order model, the melting temperature $T'(^\circ C)$ of each mixture is calculated. Thus, a 100% silica (SiO_2) mixture has its liquidus at $T'(^\circ C) = 1708.78$ according to the model versus $T(^\circ C) = 1723$ according to Grynberg [7]. Similarly, a mixture with 100% Sodium oxide (Na_2O) has its liquidus at $T'(^\circ C) = 1131.57$ according to the model versus $T(^\circ C) = 1132$ according to Zhan Zhang [4] [5]. Also, a 100% Calcium oxide (CaO) mixture has its liquidus at $T'(^\circ C) = 2570.36$ according to the model versus $T(^\circ C) = 2570$ according to Clifton [2]. A statistical study is then carried out to assess the accuracy of the model.

3.2.5. Statistical Results of the Complete Third-Order Model

The model was used to calculate liquidus values from the starting mixtures. Using the calculated values and those taken from the literature, we carry out a statistical study. Table 2 below summarizes the data used to study the accuracy of the full third-order model.

Table 2. Theoretical validation data for the complete 3-order model.

N°	SiO_2	Na_2O	CaO	$T(^\circ C)$	$\hat{T}_{3,C}(^\circ C)$	$\hat{T}_{3,C}(^\circ C)/T(^\circ C)$
1	0.74	0.2	0.06	1450	1491.43	1.03
2	0.78	0.11	0.11	1450	1352.11	0.93
3	0.39	0.21	0.4	1425	1221.35	0.86
4	0.8	0.1	0.1	1500	1357.96	0.91
5	0.39	0.2	0.41	1428	1214.49	0.85
6	0.44	0.07	0.5	1330	1403.01	1.05
7	0.45	0.07	0.48	1305	1375.46	1.05
8	0.74	0.13	0.13	1450	1351.01	0.93
9	0.75	0.15	0.1	1500	1410.54	0.94

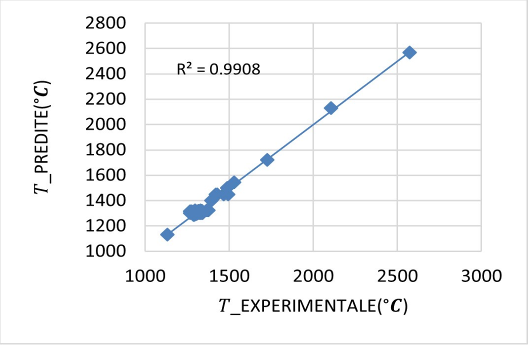

Figure 9. Correlation of predicted and experimental melting temperatures of mixtures.

The correlation between the predicted (estimated) melting temperature and the experimental melting temperature of each mixture is shown in Figure 9. The coefficient of determination of the polynomial $\hat{T}_{3,C}\left({}^{\circ}\mathrm{C}\right)$ is $R^2 = 0.9908$. This value of the coefficient is greater than the reference ($R^2 = 0.9908 > 0.9500$) and represents the highest result obtained. The formula provided in Section 2.4 and the appendix outlines the calculation procedure

3.3. Complete Third-Order Model Test

The third-order mathematical model established above was calibrated. An experimental phase dedicated to verifying the model's predictions. Test mixes are melted in the mechanics and materials science laboratory using two Nabertherm furnaces. The compositions of the test mixes are generated using the model and their melting temperature. Table 3 below summarizes the test mixes.

Table 3. Compositions of test mixtures.

N°	SiO_2	Na_2O	CaO	$T\left({}^{\circ}\mathrm{C}\right)$
1	0.210 (42 g)	0.485 (97 g)	0.305 (61 g)	$T = 1239$
2	0.215 (43 g)	0.480 (96 g)	0.335 (67 g)	$T = 1209$
3	0.200 (40 g)	0.490 (98 g)	0.310 (62 g)	$T = 1203$

Using the complete third-order model, an illustration of the ternary diagram of the SiO_2-Na_2O-CaO system is proposed.

3.4. Ternary Diagram

Figure 10 and Figure 11 are illustrations of the ternary diagram of the SiO_2-Na_2O-CaO system obtained using the full third-order model.

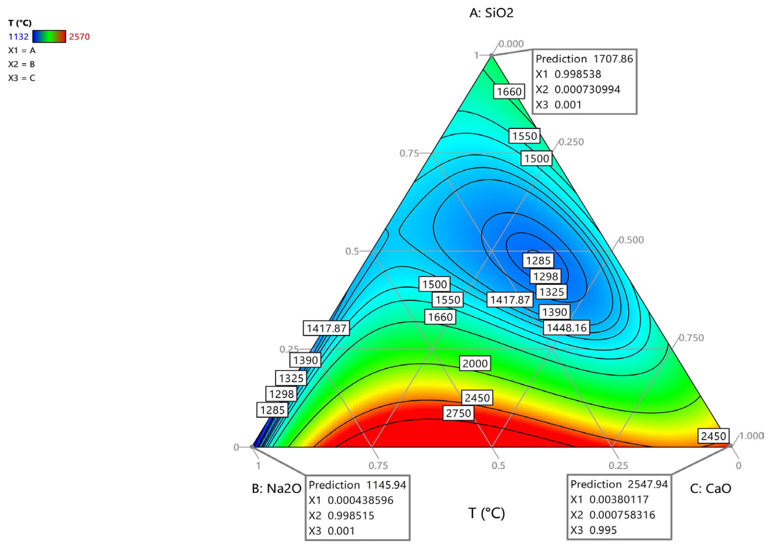

Figure 10. Ternary diagram of the SiO_2-Na_2O-CaO ternary system of the full 3-order model.

Continuous lines are shown in this diagram. They represent liquidus of mixtures whose compositions coincide with these. Red indicates very high temperatures of around 2570˚C.

However, blue indicates a temperature of 1132˚C. So, the color gradient observed on the diagram is similar to the temperature of the liquidus of the mixtures.

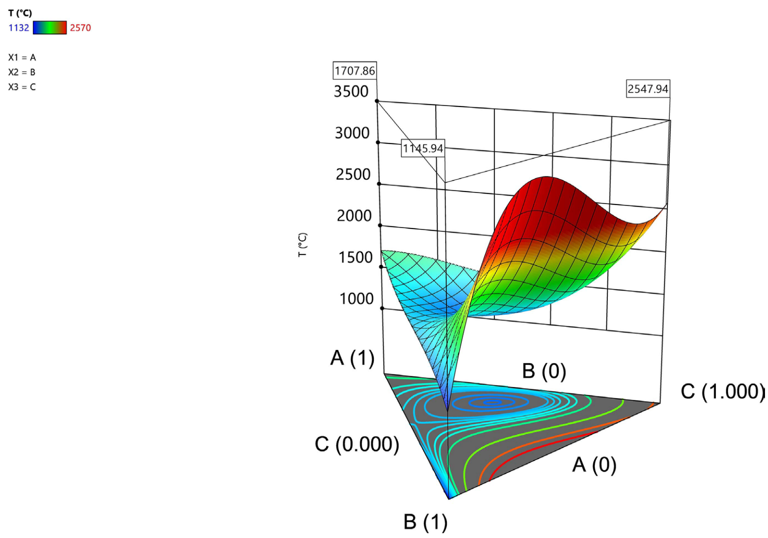

Figure 11. 3D ternary diagram of the SiO_2-Na_2O-CaO ternary system of the full 3-order model.

3.5. Melt Tests and Micrography of Test Samples

The test samples resulted in the formation of a glass paste. Due to the high content of sodium carbonate (flux) in the composition of the samples, there was good melting of the mixtures [19].

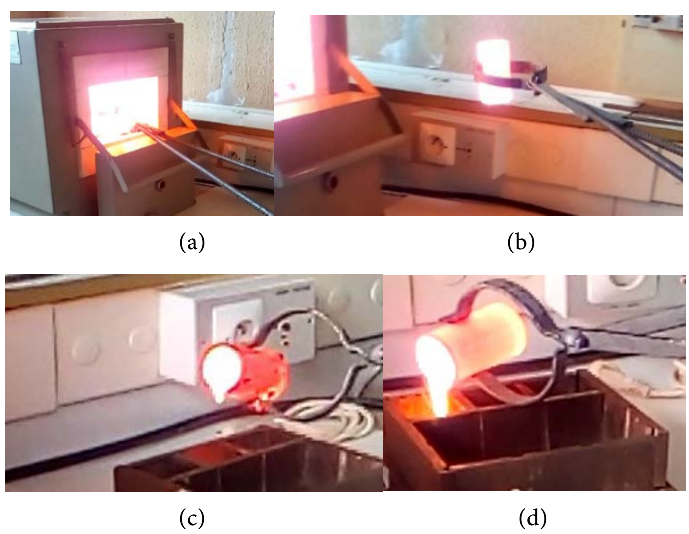

Figure 12. Glass paste pouring stage. (a) and (b) recovery of the crucibles inside the furnace, (c) pouring of the glass paste into an iron mold and (d) end of the leg pouring.

The casting of each glass pastes enabled samples of soda-lime glass to be obtained easily. Figure 12 above illustrates the casting of the glass pastes obtained.

Once the cast glass melt has cooled, the samples obtained are described. The glass samples of the test mixtures are micrographed to provide a better view of the melting state. Figure 13 below shows the degree of melting of the blends.

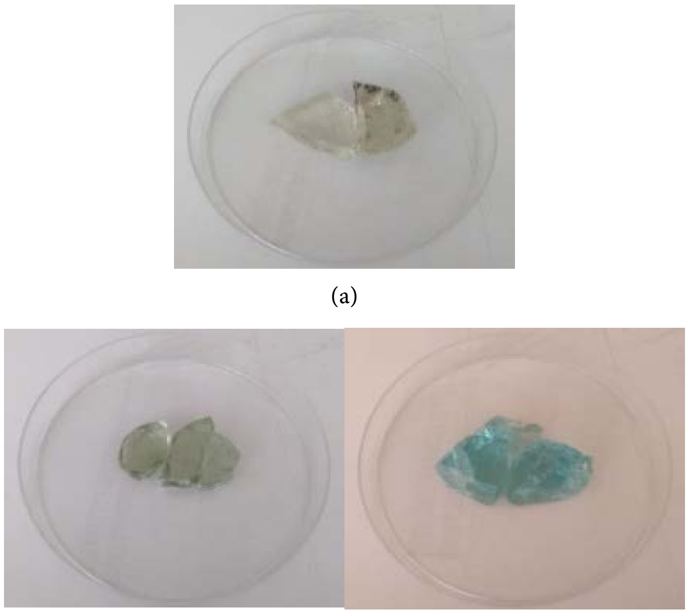

(a)

(b) (c)

Figure 13. Glass samples produced from vitrifiable test mixes. (a) mix 1 from Table 3; (b) mix 2 from Table 3 and (c) mix 3 from Table 3.

Overall, the predicted liquidus resulted in a significant degree of melting, making glass melt casting feasible. However, all produced glass samples contained trapped un-melted particles. Despite this, the findings justify maintaining the complete third-order model, based on its accuracy (R^2 = 0.9908), even though it remains insufficient. Further studies are being carried out to develop a more predictive model. Series of tests need to be carried out for an adjustment of the coefficients $b_i, b_{ij}, \delta_{ij}, b_{ijk} \in \mathbb{R}$ in order to improve the accuracy of said model. The presence of unmelted particles can be linked to several factors. Firstly, some quartz grains in the mixture may exceed 200 micrometers in size, as indicated by Emmanuelle Gouillart [8]. In addition, the temperature may be insufficient to achieve complete melting of each batch of samples, according to J. Barton's work [18]. From another perspective, unmelted particles may persist due to the mixture's composition, particularly the proportion of flux. These hypotheses help explain the presence of unmelted particles.

4. Conclusion

This mathematical approach, followed by the experimental approach, has resulted in a model for estimating the liquidus of SiO_2-Na_2O-CaO ternary mixtures. The accuracy of this model ($R^2 = 0.9908$) was assessed by means of melting tests. Using the predictive model obtained, a ternary diagram was proposed to facilitate the determination of liquidus as a function of blend compositions. An algorithm based on this model was also developed for ease of use. Also, the production phase of doped silica glass samples for wavelength transmission studies can be started on the basis of this model. However, further studies could be carried out to address the presence of unmelted particles in the glass samples after melting the ternary SiO_2-Na_2O-CaO mixture.

Conflicts of Interest

The authors declare no conflicts of interest regarding the publication of this paper.

References

[1] Haase, R. (1963) Thermodynamik der Irreversiblen Prozesse. Springer, 2.

[2] Clifton, S.H.R. and Bergeron, G. (1984) Introduction to Phase Equilibria in Leramics. The American Ceramic Society. (In English)

[3] David, W.E.L. and Richerson, W. (2018) Modern Ceramic Engineering: Properties, Processing, and Use in Design. CRC Press, 837.

[4] Zhang, Y.X.Z. and Voncken, J. (2012) Thermodynamic Assessment of the CaO-Na_2O-SiO_2 Slag System. *Ninth International Conference on Molten Slags*, *Fluxes and Salts*, Beijing, 28-31 May 2012, 11.

[5] Zhang, Z., Xiao, Y., Voncken, J., Yang, Y., Boom, R., Wang, N., *et al.* (2011) Phase Equilibria in the Na_2O-CaO-SiO_2 System. *Journal of the American Ceramic Society*, **94**, 3088-3093. https://doi.org/10.1111/j.1551-2916.2011.04442.x

[6] Schairer, J.F. (1957) Melting Relations of the Common Rock-Forming Oxides. *Journal of the American Ceramic Society*, **40**, 215-235. https://doi.org/10.1111/j.1151-2916.1957.tb12608.x

[7] Grynberg, J. (2012) Mécanismes physiques et chimiques mis en jeu lors de la fusion du mélange SiO_2-Na_2CO_3. Master's Thesis, Université Pierre et Marie Curie-Paris VI. (In Français) https://tel.archives-ouvertes.fr/tel-00829455

[8] Gouillart, E., Toplis, M.J., Grynberg, J., Chopinet, M., Sondergard, E., Salvo, L., *et al.* (2012) *In Situ* Synchrotron Microtomography Reveals Multiple Reaction Pathways during Soda-lime Glass Synthesis. *Journal of the American Ceramic Society*, **95**, 1504-1507. https://doi.org/10.1111/j.1551-2916.2012.05151.x

[9] Tinsson, W. (2010) Plans d'expérience: Constructions et analyses statistiques, Mathématiques et Applications. Springer-Verlag, 535.

[10] Gendre, L., Savary, A. and Soulier, B. (2009) Les plans d'expériences. Edusolsti Sienscachan, 14. http://eduscol.education.fr/sti/si-ens-cachan/

[11] Goupy, J. (2006) Les plans d'expériences. *Revue Modulad*, **34**, 74-116.

[12] Ghawaly, J.M., Nicholson, A.D., Peplow, D.E., Anderson-Cook, C.M., Myers, K.L., Archer, D.E., *et al.* (2020) Data for Training and Testing Radiation Detection Algorithms in an Urban Environment. *Scientific Data*, **7**, Article No. 328. https://doi.org/10.1038/s41597-020-00672-2

[13] Sugali, K., Sprunger, C. and N Inukollu, V. (2021) AI Testing: Ensuring a Good Data Split between Data Sets (Training and Test) Using K-Means Clustering and Decision Tree Analysis. *International Journal on Soft Computing*, **12**, 1-11.

https://doi.org/10.5121/ijsc.2021.12101

[14] Gholamy, A., Kreinovich, V. and Kosheleva, O. (2018) Why 70/30 or 80/20 Relation between Training and Testing Sets: A Pedagogical Explanation. Departmental Technical Reports (CS). https://scholarworks.utep.edu/cs_techrep/1209

[15] Thio, R.P., Konan, D.K., Koffi, B.K. and Yao, A.K. (2020) Characterization of Raw Silica Sand from the Ivorian Sedimentary Basin for Silica Glass Making. *Journal of Materials and Environmental Science*, **11**, 2016-2024.

[16] Thio, P.R., Koffi, K.B., Konan, K.D. and Yao, K.A. (2021) Production of High-Purity Silica Sand from Ivorian Sedimentary Basin by Attrition without Acid Leaching Process for Windows Glass Making. *Journal of Minerals and Materials Characterization and Engineering*, **9**, 345-361. https://doi.org/10.4236/jmmce.2021.94024

[17] Daud, M. and Abu Hassan, M. (2014) Preparation and Characterization of Soft Glass Using Sarawak Silica Sand as Starting Material for Craftware. *Advanced Materials Research*, **895**, 363-374. https://doi.org/10.4028/www.scientific.net/amr.895.363

[18] Barton, J. and Guillemet, C. (2005) Le verre: Science et technologie. EDP Sciences: chimie matériaux, 461.

[19] Rafi, A.S.M.M., Tasnim, U.F. and Rahman, M.S. (2018) Quantification and Qualification of Silica Sand Extracted from Padma River Sand. *IOP Conference Series*: *Materials Science and Engineering*, **438**, Article ID: 012037. https://doi.org/10.1088/1757-899x/438/1/012037

Appendix: Python Algorithm for the Complete 3rd-Order Model

```
from sklearn.model_selection import train_test_split
import numpy as np
from scipy import stats

# data set
```

$$x, y = \text{np.array}\left(\begin{bmatrix} & \cdots & \\ \vdots & \ddots & \vdots \\ & \cdots & \end{bmatrix}\right), \text{np.array}\left(\begin{bmatrix} & \cdots & \\ \vdots & \ddots & \vdots \\ & \cdots & \end{bmatrix}\right)$$

```
# Determine desired size of drive assembly (rounded)
# 80% of dataset
total_samples = len(x)
desired_train_size = round(total_samples * 0.8)

# Round off the size of the drive assembly
if total_samples - desired_train_size >= 0.5:
    train_size = desired_train_size
else:
    train_size = desired_train_size + 1

# Separate drive and validation assemblies
x_train, x_val, y_train, y_val = train_test_split(x, y, train_size=train_size, random_state ∈ ℕ*)

M = x_train.T.dot(x_train)
matrice_inverse = np.linalg.inv(M)
M2 = x_train.T.dot(y_train)

theta = matrice_inverse.dot(M2)

# model

def model(x_train, theta):
    return x_train.dot(theta)

predictions = model(x_train, theta)

def coef_determination(y_train, predictions) :

    u= ((y_train-predictions)**2).sum()
    v= ((y_train-y_train.mean())**2).sum()
```

```
    return 1 - u/v
R_carré = coef_determination(y_train, predictions)

# freedom degrees
n = len(y_train)    # Nombre d'observations
p = len(theta)       # Nombre de variables explicatives (coefficients)

# residuals squares sum
residuals = y_train - predictions
sse = np.sum(residuals ** 2)

# explained squares sum
mean_y = np.mean(y_train)
ssr = np.sum((predictions - mean_y) ** 2)

# descriptive statistics
f_statistic = (ssr / p) / (sse / (n - p - 1))

# Calcul de la p-value associée
p_value = 1 - stats.f.cdf(f_statistic, p, n - p - 1)

# Affichage des résultats
print("Statistique F:", f_statistic)
print("P-value:", p_value)
```